Combustion and Flame 162 (2015) 1712–1718

Contents lists available at ScienceDirect

Combustion and Flame

journal homepage: www.elsevier.com/locate/combustflame

Near-lean limit combustion regimes of low-Lewis-number stretched premixed flames

Roman Fursenko [a,d,*], Sergey Minaev [a,d], Hisashi Nakamura [b], Takuya Tezuka [b], Susumu Hasegawa [b], Tomoya Kobayashi [b], Koichi Takase [b], Masato Katsuta [c], Masao Kikuchi [c], Kaoru Maruta [b,d]

[a] Khristianovich Institute of Theoretical and Applied Mechanics, SB RAS, 4/1, Institutskaya Str., Novosibirsk 630090, Russia
[b] Institute of Fluid Science, Tohoku University, 2-1-1 Katahira, Aoba, Sendai 980-8577, Japan
[c] Tsukuba Space Center, Japan Aerospace Exploration Agency, Sengen, Tsukuba, Ibaraki 305-8505, Japan
[d] Far Eastern Federal University, 8, Sukhanova Str., Vladivostok 690950, Russia

ARTICLE INFO

Article history:
Received 1 July 2014
Received in revised form 14 November 2014
Accepted 25 November 2014
Available online 31 December 2014

Keywords:
Counterflow premixed flames
Cellular flames
Heat loss
Flame ball
Diffusive-thermal instability

ABSTRACT

Dynamic behavior and 3D spatial structure of low-Lewis-number counterflow premixed flames are numerically studied in the frame of thermo-diffusive model with one-step chemical reaction. The diverse combustion regimes are described and regions of existence of these regimes in equivalence ratio/stretch rate plane are identified. Qualitative comparison between numerical results and results of microgravity experiments are discussed. Experiments and numerical simulations demonstrate that at small stretch rate conditions lean low-Lewis-number counterflow flames can appear as a set of separate ball-like flames in a state of chaotic motion. The extension of extinction limits associated with existence of sporadic combustion regimes is observed.

1. Introduction

Although extensive literature on flammability limits of stretched premixed flames exists, the detailed understanding of near-limit low-Lewis-number flames phenomena is still necessary. The extinction limits of counterflow methane–air flames within the range of Lewis numbers from 0.97 to 1.8 were studied in [1–7]. Within this range, the distribution of stretch rate versus equivalence ratio gives the flammability boundary curve. Taking into account the range of parameters when the normal and weak flames can exist, this curve has G-shape [1,3]. Numerical simulations and linear stability [5] analysis for these regimes are conducted using one-dimensional models. At low Lewis numbers latest predict the existence of C-shape flammability curve for hydrogen–air flames, while experiments show that at low stretch rates the flame can exist below predicted flammability limit. For instance, low Lewis number flame front can be non-planar and can assume variety of possible spatial patterns such as flame tubes and cellular flame [8]. In the case of low Lewis numbers the planar flame is spatially unstable due to the diffusive-thermal instability which cannot be described correctly using one-dimensional approach and multi-dimensional models are required.

Using two and three-dimensional models it was found that under the intensive heat loss the flame propagating in straight [9,10] and divergent [11] channels break up on separate moving flame cells. In some cases [9,10] these separate fragments have almost spherical form resembling "flame balls" which were found in microgravity experiments [12,13]. It is interesting, that at normal gravity such structures can be observed sometimes when the flame propagates in vertical tube [14]. Recent experiments for counterflow flames under microgravity conditions [15,16] have demonstrated the existence of ball-like and cellular structures. Such structures were termed as "sporadic combustion wave" [15].

Due to a high complexity related with detailed chemical kinetics [17,18], transport processes and radiative heat losses, the direct numerical simulations of non-planar stretch flames is difficult and requires a high computational load in order to resolve spatiotemporal structure of sporadic combustion wave [19]. In the present study, we apply reduced three-dimensional reaction–diffusion model in order to investigate qualitative behavior of near-limit low-Lewis-number counterflow flames for a wide range of problem parameters. Although this model is simplified, it describes qualitatively main features of counterflow flames under microgravity conditions

* Corresponding author at: Khristianovich Institute of Theoretical and Applied Mechanics, Siberian Branch of Russian Academy of Sciences, 4/1, Institutskaya Str., Novosibirsk 630090, Russia. Fax: +7 (383) 3307268.
E-mail address: roman.fursenko@gmail.com (R. Fursenko).

http://dx.doi.org/10.1016/j.combustflame.2014.11.032
0010-2180/

[15] consisting of separate ball-like flames in a state of chaotic motion. We have to note that such structures cannot be observed under normal gravity due to the buoyancy effect [1,2,20,21]. In this work we extend our previous results for the wide range of near flammability limits combustion regimes of stretched flames.

2. Experimental setup

A schematic of the experimental setup is shown in Fig. 1. A pair of 3 cm diameter counterflow burners is enclosed in a chamber. The distance between the burner lips is 3 cm. The burners are made of brazen circular pipes with a porous plate inside and designed so that nearly flat flow velocity profiles are ensured at low flow rates. The control system consists of a PC, mass flow controllers, AD/DA converters and a trigger circuit. The stretch rate $\alpha = U/L$ is maintained at a constant value, where U is the flow velocity at the burner outlet and L is the burner distance. The mixture consists of CH_4, O_2 and Xe. The ratio of the O_2 and Xe mole fractions is fixed to $X_{O2}/X_{Xe} = 0.141$, while the concentration of CH_4 was regulated in such a way that the equivalence ratio decreased linearly and gradually with time within 0.65–0.3 range. For the given mixtures the Lewis number is around 0.5.

The microgravity conditions are obtained during parabolic flights of MU300 jet airplane operated by the Diamond Air Service Company [22]. Overall duration of the microgravity is around 20 s. The flow velocity at the burner exit and mixture composition for each experiment is assigned several seconds before the start of microgravity. The mixture is ignited by a pilot flame and the pilot flame is removed after the start of microgravity. The equivalence ratio is gradually decreased during the microgravity conditions. The flame behavior is observed with two video cameras which are mounted perpendicular to the burner axis and each other. One camera is equipped with an image intensifier.

Accuracy of the airplane microgravity conditions is verified by comparison of the present data with those obtained in JAMIC (Drop tower) experiments [21]. The airplane and drop tower experimental data were found to be in good agreement and the difference in equivalence ratios at extinction was less than 3% for stretch rates 3–11 1/s.

3. Mathematical model

Three-dimensional model of counterflow premixed flames is considered. The air–fuel mixture is supplied from two opposite burners located at positions $y = \pm L_y$, so that the stagnation flow plane coincides with $X0Z$ one. In the framework of our model, the following approximations are made: one-step Arrhenius type exothermic reaction with single reactant, fuel lean mixtures, constant density, constant diffusion transport coefficients, simplified representation of radiative heat loss. Under these assumptions, the non-dimensional equations describing temperature and fuel concentration fields can be written as follows:

$$T_t + \vec{V}\cdot\nabla T = \nabla^2 T - h(T^4 - \sigma^4) + (1-\sigma)W(T,C), \quad (1)$$

$$C_t + \vec{V}\cdot\nabla C = Le^{-1}\nabla^2 C - W(T,C), \quad (2)$$

Here T is the temperature in units of the adiabatic temperature of combustion products, T_b, C is the fuel concentration in units of that for the fresh mixture, C_0. The velocity is measured in units of the velocity of a planar adiabatic flame in the high activation energy limit, U_b, the distance in the units of the thermal width of flame $l_{th} = D_{th}/U_b$, where D_{th} is the thermal diffusivity of the mixture. So that the time is measured in units D_{th}/U_b^2. The dimensionless initial temperature is denoted by $\sigma = T_0/T_b$. The Lewis number is $Le = D_{th}/D_{mol}$, where D_{mol} is the fuel molecular diffusivity. The dimensionless

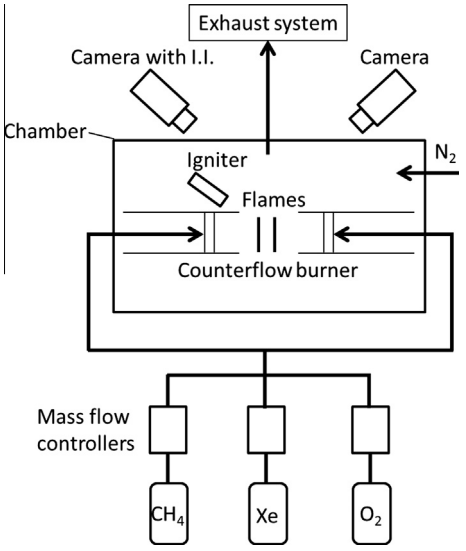

Fig. 1. Schematic of experimental system.

flow velocity vector is given by $\vec{V} = (ax/2, -ay, az/2)$, where a is the non-dimensional stretch rate in units U_b^2/D_{th}. Chemical reaction rate has the following form $W(T,C) = \frac{C}{2Le}(1-\sigma)^2 N^2 \exp(N(1-1/T))$, where non-dimensional activation temperature $N = T_a/T_b = \sigma T_a/T_0$ is the ratio of activation temperature T_a and adiabatic flame temperature T_b. Formula for adiabatic flame speed in the high activation energy limit reads $U_b = B\exp(-N/2) = B\exp(-T_a/2T_b)$. In these variables, the velocity of the planar adiabatic flame tends to unity at large N. The activation temperature T_a and pre-exponential factor B in above formula were chosen to fit the dependence of U_b on adiabatic flame temperature T_b obtained by using relations $T_b(\phi)$ and $U_b(\phi)$ which were calculated by the detailed reaction mechanism GRI-Mech 3.0 in the range of lean mixtures with equivalence ratio $\phi < 0.8$. The second term in the right-hand side of Eq. (1) describes radiative heat loss. Following [5,6] we assume that gas irradiation is mainly caused by the emission of the combustion products and, therefore, the dimensional radiation heat loss coefficient $h_{dim} \sim hU_b^2/D_{th}$ is proportional to the concentration of the deficient reactant C_0. Since $U_b^2 \sim \exp(-N)$ and $C_0 \sim (1/\sigma - 1)$ the scaled Stefan–Boltzmann constant h in Eq. (2) can be expressed as $h = A(1-\sigma)/\sigma\exp(N)$, where A is non-dimensional parameter in units of $\rho_b c_p l_p U_b/4T_b^3 l_{th}$, l_p is the Planck absorption length; c_p is the specific heat, ρ_b is the gas density. The value of parameter $A = 3.69\cdot 10^{-7}$ is chosen to match the flammability limit of the lean planar flame.

Eqs. (1) and (2) are considered in the rectangular domain $-L_x \leqslant x \leqslant L_x$, $-L_y \leqslant y \leqslant L_y$, $-L_z \leqslant z \leqslant L_z$ and following boundary conditions are applied

$$\text{Inlet } (y = \pm L_y): T = \sigma; C = 1, \quad (3)$$

$$x = \pm L_x, z = \pm L_z: T = \sigma; C = 0. \quad (4)$$

At the initial moment, the computational domain is filled by fresh mixture with temperature σ. The flame is ignited by specifying the high temperature zone $-L_x < x_0 \leqslant x \leqslant x_1 < L_x$, $-L_y < y_0 \leqslant y \leqslant y_1 < L_y$, $-L_z < z_0 \leqslant z \leqslant z_1 < L_z$ near the stagnation plane.

The set of governing Eqs. (1) and (2) with boundary conditions (3) and (4) is solved numerically by explicit finite-difference scheme on the orthogonal grid. In order to check the convergence of the numerical scheme, simulations of the stationary adiabatic flame and sporadic combustion wave [15] were performed with the different spatial resolutions. The following grids $256\times192\times256$, $320\times240\times320$, $384\times288\times384$, 400×304